Mon. Not. R. Astron. Soc. **000**, 000–000 (0000) Printed 1 February 2008 (MN LATEX style file v1.4)

An XMM-Newton observation of the extreme Narrow Line Seyfert 1 Galaxy, Mrk 359

P.T. O'Brien,[1] K. Page,[1] J.N. Reeves,[1] K. Pounds,[1] M.J.L. Turner,[1] E.M. Puchnarewicz[2]

[1] *X-ray Astronomy Group, Department of Physics and Astronomy, University of Leicester, LE1 7RH, U.K.*
[2] *Mullard Space Science Laboratory, University College London, Holmbury St. Mary, Dorking, Surrey, RH5 6NT, UK*

2001 June

ABSTRACT

We present *XMM-Newton* observations of Mrk 359, the first Narrow Line Seyfert 1 galaxy discovered. Even among NLS1s, Mrk 359 is an extreme case with extraordinarily narrow optical emission lines. The *XMM-Newton* data show that Mrk 359 has a significant soft X-ray excess which displays only weak absorption and emission features. The (2–10) keV continuum, including reflection, is flatter than the typical NLS1, with $\Gamma \approx 1.84$. A strong emission line of equivalent width ≈ 200 eV is also observed, centred near 6.4 keV. We fit this emission with two line components of approximately equal strength: a broad iron-line from an accretion disc and a narrow, unresolved core. The unresolved line core has an equivalent width of ≈ 120 eV and is consistent with fluorescence from neutral iron in distant reprocessing gas, possibly in the form of a 'molecular torus'. Comparison of the narrow-line strengths in Mrk 359 and other low–moderate luminosity Seyfert 1 galaxies with those in QSOs suggests that the solid angle subtended by the distant reprocessing gas decreases with increasing AGN luminosity.

Key words: galaxies: galaxies: active – galaxies: individual: Mrk 359 – accretion, accretion discs – X-rays: galaxies.

1 INTRODUCTION

Exploring the extremes of parameter space is an invaluable way of probing the physical processes occurring in any class of astronomical object. We adopt this approach here and discuss the *XMM-Newton* X-ray spectra of the nearby Seyfert 1 galaxy Mrk 359 ($z = 0.0174$). Davidson & Kinman (1978) noted that lines from both the Narrow Line Region (NLR) and the Broad Line Region (BLR) are unusually narrow in Mrk 359. They also noted the presence of strong high-ionisation lines and suggested Mrk 359 merited further study. The narrowness of the emission lines combined with the presence of strong high-ionisation lines led Osterbrock & Dahari (1983) to classify Mrk 359 as a Narrow Line Seyfert 1 galaxy (NLS1), the first such object discovered. Veilleux (1991) found that the FWHM of the forbidden lines (NLR) is ≈ 135 km s^{-1} while the permitted lines (BLR) have FWHM ≈ 800 km s^{-1}. Even for NLS1s, these are extraordinarily narrow line widths. Both the NLR and BLR profiles are also unusual among the sample studied by Veilleux in that they show no substructure.

NLS1s have become a prime target for X-ray observation due to their extreme variability characteristics and unusual spectral shape (e.g. Boller, Brandt & Fink 1996). Mrk 359 has relatively little previous X-ray data. It was first detected during the *Einstein* slew survey (Elvis et al. 1992). Assuming it has a 'normal' 2–10 keV spectral index, Walter & Fink (1993) suggest Mrk 359 has a moderately strong soft X-ray excess based on the *ROSAT* all sky survey data. Boller et al. (1996) found it had a fairly flat continuum for the NLS1 class in the *ROSAT* bandpass ($\Gamma = 2.4 \pm 0.1$).

In this paper we present *XMM-Newton* observations of Mrk 359. Due to the combination of the broad bandpass, spectral resolution and high throughput of the *XMM-Newton* instrumentation, these data are a considerable improvement on previous observations. We find strong line emission, centred at 6.4 keV in the rest-frame of Mrk 359, superimposed on a type-1 AGN continuum consisting of a high-energy powerlaw and a strong soft X-ray excess.

2 XMM-NEWTON OBSERVATIONS

Although actually a guaranteed time target, Mrk 359 was observed in revolution 107 (9 July 2000) during the early calibration and performance verification phase of the mission. The European Photon Imaging Camera (EPIC) PN (Strüder et al. 2001) and EPIC MOS (Turner et al. 2001)

Table 1. Fits to *XMM-Newton* 2–10 keV data for Mrk 359. [a]Excluding 5.5–7 keV region. [b]Rest-frame energy of emission line (intrinsic line-width, $\sigma < 0.08$ keV).

Camera	Fit	Model	Γ	E[b] (keV)	χ^2/dof
MOS	1[a]	PL	1.77 ± 0.09	–	56/69
PN	1[a]	PL	1.91 ± 0.05	–	164/167
MOS+PN	1[a]	PL	1.88 ± 0.04	–	223/237
PN	2	PL+GA	1.88 ± 0.04	6.41 ± 0.05	190/192
MOS+PN	2	PL+GA	1.85 ± 0.04	6.43 ± 0.03	259/270

exposure times were 7.3 and 4 kecs respectively. The Reflection Grating Spectrograph (RGS; den Herder et al. 2001) exposure time was 27 ksecs.

The EPIC MOS and PN cameras were operated in full-frame observing mode using the medium filters. Event lists output from the standard EMCHAIN and EPCHAIN scripts were further filtered using the SAS (Science Analysis Software) XMMSELECT task. Only X-ray events corresponding to patterns 0–12 (similar to *ASCA* event grades 0–4) were selected for the MOS exposures. For the PN patterns 0–4 (singles and doubles) were used. Hot pixels and electronic noise were rejected during data processing and the low-energy cut-off for spectral extraction was set at 200 eV.

Source spectra were extracted from the EPIC images using a circular source region of diameter 1 arcminute centred on the observed source position. Background spectra were derived from adjacent 'blank sky' regions. Before further analysis the EPIC spectra were binned to give a minimum of 20 counts per bin. The XSPEC V11.0 software package was used to calibrate the background-subtracted EPIC spectra using the most recent camera response matrices derived from ground-based and in-orbit data. Errors on fitted parameters are quoted at the 90% confidence level.

The RGS data were processed using the standard SAS RGSPROC script and calibrated using response matrices derived using the RGSRMFGEN task.

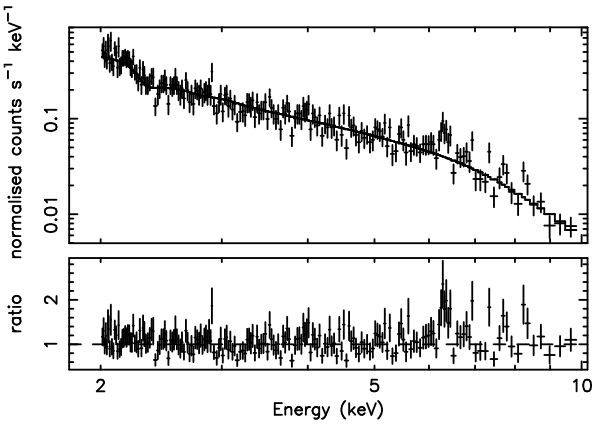

Figure 1. The 2–10 keV EPIC PN spectrum of Mrk 359 fitted with a powerlaw. The powerlaw fit excludes the region from 5.5–7 keV (fit 1 in Table 1). The lower plot shows the ratio of the fitted powerlaw to the data.

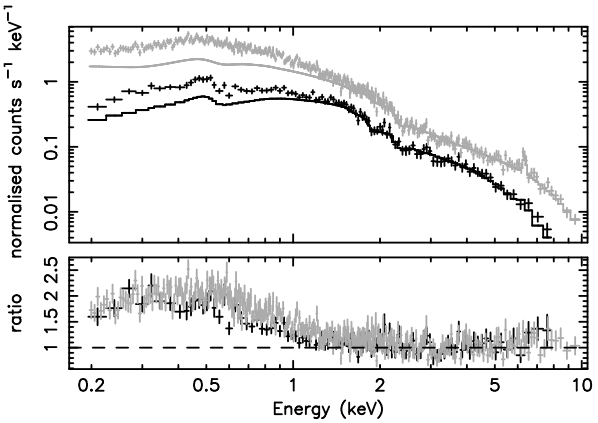

Figure 2. The 0.2–10 keV EPIC MOS and PN spectra of Mrk 359. The extrapolated 2–10 keV powerlaw+Gaussian line model (fit 2 in Table 1) is also shown. A strong soft excess is present below ≈ 2 keV.

3 SPECTRAL ANALYSIS

As usual with AGN, the first model fitted to Mrk 359 was that of a single absorbed powerlaw. The absorbing column density was fixed at the Galactic value of $N_h = 4.79 \times 10^{20}$ cm^{-2}. Fitting to the joint EPIC MOS+PN data over the entire 0.2–10 keV bandpass provides a poor fit ($\chi^2_\nu = 1097/743$). To examine the detailed spectral shape, the fitting procedure was therefore split in two, first fitting over 2–10 keV and then over the broad-band 0.2–10 keV.

3.1 The 2–10 keV spectrum

A powerlaw was fitted over 2–10 keV excluding the iron line region (5.5–7 keV). This fit, called fit 1 in Table 1, provides an acceptable fit to either the MOS or PN data separately or when combined (e.g., $\chi^2_\nu = 0.93$ for MOS+PN) giving a photon index $\Gamma \approx 1.9$. Fit 1 for the PN is shown in Fig. 1.

A clear 'feature' is seen near 6.4 keV in the PN data (Fig. 1), so a Gaussian emission line was added (fit 2 in Table 1). This significantly improves the fit compared to that of a powerlaw fitted over the entire 2–10 keV band ($\Delta\chi^2 = 23$ for 3 additional parameters). The emission line is not well defined in the MOS data, but using both datasets gives a fit statistically consistent to that of the PN alone. Adding the emission line flattens the PN hard continuum slope slightly to $\Gamma = 1.88$. The rest-frame energy for the emission line in the PN spectrum is 6.41 ± 0.05 keV, consistent with that expected for fluorescence from neutral iron. The fitted Gaussian line is unresolved ($\sigma < 80$ eV) and is very strong, with an EW of 216 ± 73 eV in the PN spectrum. Adding a second Gaussian line does not improve the fit, but there are indications of a broader line component in the data residuals (Fig. 1). We discuss more detailed iron line models below.

3.2 The 0.2–10 keV spectrum

Extrapolating the best-fit 2–10 keV powerlaw (fit 2 in Table 1) back to 0.2 keV clearly reveals a broad "soft excess" in both the PN and MOS spectra (Fig. 2). To fit the broad-band spectrum, we fixed the iron-line parameters and used blackbody (BB) components to parameterise the soft excess. Using a single blackbody provides a reasonable fit to the soft emission (fit 3 in Table 2) but the powerlaw slope steepens. Using two blackbodies significantly improves the fit ($\Delta\chi^2 =$

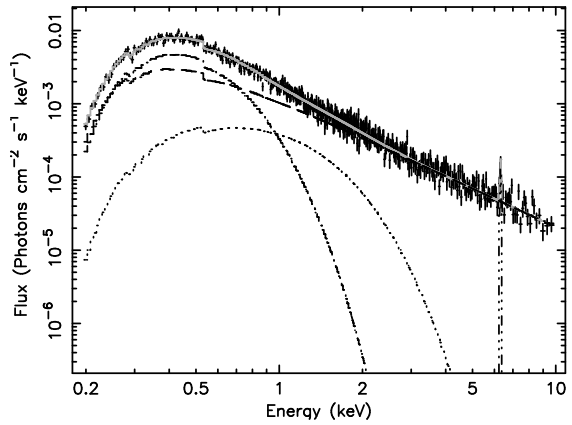

Figure 3. The unfolded 0.2–10 keV EPIC PN spectrum of Mrk 359 fitted using a powerlaw, two blackbodies and a Gaussian emission line (fit 4 in Table 2).

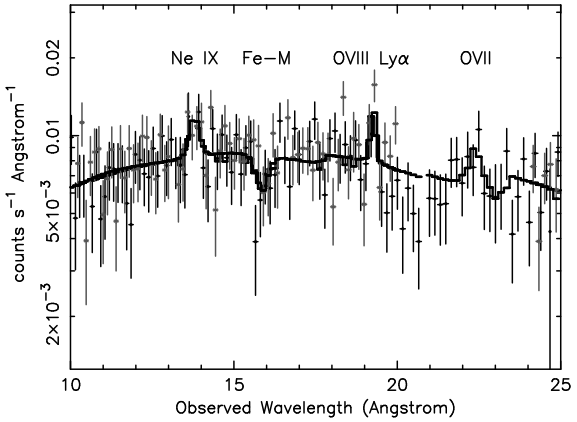

Figure 4. The RGS spectrum of Mrk 359 showing the significant spectral features. See text for details.

20 for 2 additional parameters; fit 4 in Table 2) and hardens the fitted powerlaw. The unfolded spectrum corresponding to fit 4 is shown in Fig. 3.

Using fit 4 in Table 2, the 0.2–10 keV flux of Mrk 359 is 1.26×10^{-11} erg cm^{-2} s^{-1}, corresponding to a luminosity of 1.7×10^{43} erg s^{-1} (assuming $H_0 = 50$ km s^{-1} Mpc^{-1} and $q_0 = 0$). Most of this luminosity, 1.0×10^{43} erg s^{-1}, is in the 0.2–2 keV band, distributed equally between the powerlaw and multiple blackbody components. The 2–10 keV luminosity of 7.0×10^{42} erg s^{-1} is dominated by the powerlaw component in the fit.

The soft X-ray luminosity of Mrk 359 during the *XMM-Newton* observation was more than a factor of two lower than the luminosity derived by Boller et al. (1996) from the 15 July 1992 *ROSAT* data. They note, however, that Mrk 359 varied by a factor of 1.5 in just 10 hours. Fitting a powerlaw to the *XMM-Newton* data over the 0.2–2.4 keV band gives $\Gamma = 2.34 \pm 0.02$, identical to the value of 2.4 ± 0.1 derived from the *ROSAT* data. Thus, although somewhat fainter, we have no evidence for spectral shape changes in Mrk 359 over a timescale of eight years.

No large amplitude continuum variability was seen during the RGS observation, but the continuum did vary by ±15% on timescales of several thousand seconds. This behaviour is consistent with that of other NLS1s (e.g., Boller et al. 1996).

The RGS spectrum is of relatively low S/N, but the overall shape is consistent with that of the EPIC spectra. No significant neutral intrinsic absorption is detected (intrinsic $N_h < 1.24 \times 10^{20}$ cm^{-2}) nor evidence for a 'conventional warm absorber', with limits on the O VII and O VIII edge optical depths of $\tau < 0.1$.

A weak absorption trough is detected centred at 15.6 ± 0.1 Å (rest-frame) with an EW = 6.5 ± 3.0 eV (Fig. 4), similar in location and strength to those seen in IRAS 13349+2438 (Sako et al. 2001) and Mrk 509 (Pounds et al. 2001), which were attributed to absorption in iron M ions. Narrow emission features are detected at 13.55 ± 0.07 Å and 21.98 ± 0.13 Å (rest-frame) corresponding to the Ne IX and O VII triplets. The S/N is too low to resolve these features but their total EWs are 12 ± 6 eV and 6 ± 4 eV respectively. The O VIII Lyα line is also seen at 18.94 ± 0.05 Å (rest-frame), with an EW = 5.0 ± 2.5 eV. Any associated O VIII radiative recombination continuum is less than half the strength of the Lyα emission line. This ratio suggests that, as in NGC 4151 (Ogle et al. 2001), a significant fraction of the O VIII emission may come from a hot, collisional ionised rather than photoionised plasma, possibly associated with a hot medium pressure-confining the NLR clouds.

4 THE 6.4 KEV IRON EMISSION LINE

The 6.4 keV emission line in Mrk 359 appears much stronger (EW ≈ 200 eV) than the typical EW 50–100 eV for 'narrow' iron lines seen in other Seyfert 1 galaxies (e.g. Reeves et al. 2001; Yaqoob et al. 2001; Kaspi et al. 2001; Pounds et al. 2001). Attributing all of the line emission in Mrk 359 to fluoresence from cool reprocessing gas (e.g., a torus) illuminated by the central hard X-ray continuum would require that the gas subtends an unusually large solid angle (e.g. Ghisellini, Haardt & Matt 1994), for which we have no other evidence. We therefore investigated whether iron emission from an accretion disc could be contributing to the observed line, as expected in Seyfert galaxies (see Fabian et al. 2000 and references therein).

To quantify the disc contribution, we compared the Mrk 359 EPIC PN 2–10 keV data with an accretion disc model for a non-rotating black hole. The generic 'Xion' model used here is described in detail in Nayakshin, Kazanas & Kallman (2000). The 'lamppost' geometry is assumed for the illuminating hard X-ray source. The X-ray to disc luminosity ratio was fixed at 0.3, which is reasonable for the spectral energy distribution of Mrk 359. Two basic accretion disc models were considered: a 'truncated accretion disc' which produces an intrinsically narrow emission line and a 'normal accretion disc' producing a broad line.

To explain the observed emission line as an accretion disc line which is masquerading as a narrow line we must somehow remove the broad wings commonly associated with such a line. The simplest way to do this is to truncate the disc, removing the inner higher-velocity gas. Our truncated disc model is shown in Fig. 5(a). For this model $\chi^2_\nu = 189/193$. The inner and outer radii of the disc are 50 and 1000 R$_s$ (Schwarzschild radii) respectively, and the height of the X-ray source above the disc surface is 30 R$_s$.

Table 2. Fits to *XMM-Newton* 0.2–10 keV data for Mrk 359. [a]Blackbody temperature (kT). [b]Rest-frame energy of emission line. [c]Intrinsic line-width (1-sigma). [d]Fit to ionised reflection model (Nayakshin et al. 2000) – see text for details. [f]Frozen.

Camera	Fit	Model	Γ	BB_1^a (keV)	BB_2^a (keV)	E^b/σ^c (keV)	χ^2/dof
MOS+PN	3	PL+BB+GA	1.93 ± 0.02	0.131 ± 0.002	–	6.41^f / 0.01^f	775/742
MOS+PN	4	PL+2×BB+GA	1.74 ± 0.06	0.120 ± 0.003	0.310 ± 0.026	6.41^f / 0.01^f	755/740
PN	5	Xion[d]+BB+GA	1.84 ± 0.02	0.134 ± 0.003	–	6.41^f / 0.01^f	565/528

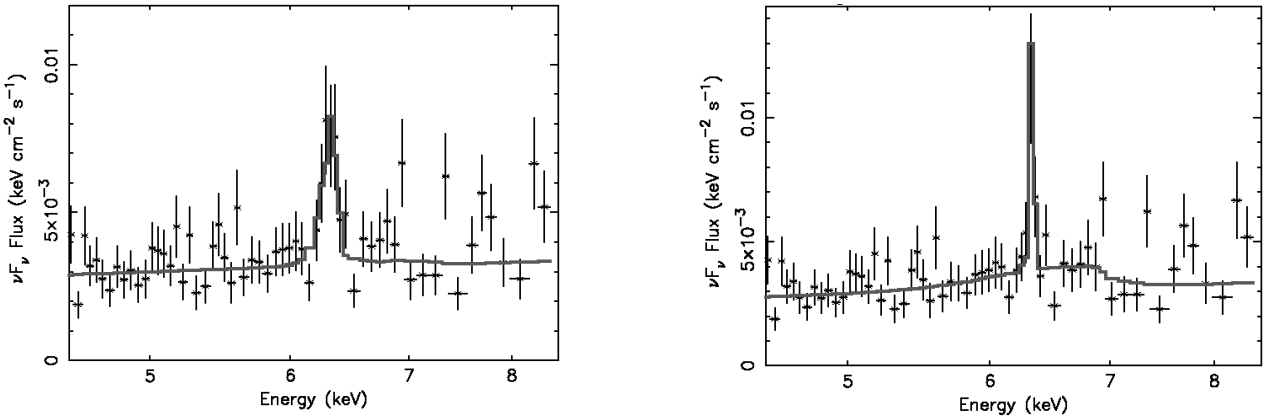

Figure 5. Accretion disc model (Nayakshin et al. 2000) fits to the 2–10 keV EPIC PN spectrum of Mrk 359. (a) face-on truncated disc with inner radius 50 R_s and accretion rate 1% Eddington plus a narrow 6.4 keV Gaussian core ($\sigma = 0.01$ keV); (b) 30 degree inclination disc extending down to 3 R_s with accretion rate 30% Eddington plus a narrow 6.4 keV Gaussian core ($\sigma = 0.01$).

The accretion rate is 0.01 Eddington. To keep the line centred at 6.4 keV, the accretion rate must be low for this model (< 0.05) in order to keep iron predominantly neutral. To explain the observed line strength requires a super-solar iron abundance, which we fixed at 5 times solar. To fit the peak of the line, the model shown in Fig. 5(a) includes an additional, narrow, unresolved Gaussian line ($\sigma = 0.01$ keV). This narrow-line component has an EW of 62 eV.

Although the truncated disc model provides a statistically acceptable fit, it does not appear physically plausible. Truncated disc models are more commonly proposed to explain soft X-ray transient (SXT) systems, a sub-class of Low mass X-ray binaries (e.g., Dubus, Hameury & Lasota 2001). These models have some similarities to those for AGN, including the possible influence of X-ray irradiation of the disc surface. However, in SXTs the disc is truncated when the system is in the 'low state', which may be inappropriate for an NLS1. As noted above, a low accretion rate is required for this model (< 0.05) to keep the iron neutral. To explain the bolometric luminosity ($\approx 10^{44}$ erg s^{-1}) such a low accretion rate implies a black hole mass $\gtrsim 10^8$ $M_\odot$. This would be a relatively high mass for a low luminosity AGN like Mrk 359 (c.f., Ferrarese et al. 2001), and is also contrary to the idea that NLS1s are relatively low-mass systems running at high accretion rates (e.g., Pounds, Done & Osborne 1995). The generic X-ray properties of NLS1s, and in particular their variability (Boller et al. 1996), strongly suggests that they have discs extending down to the minimum allowed radius (i.e., 3 R_s for a non-rotating black hole).

To avoid these difficulties, an accretion disc model in which the disc extends down to 3 R_s was calculated and is shown in Fig. 5(b). For this model $\chi^2_\nu = 187/193$. The parameters of the model are not well constrained, so we fixed the disc inclination angle at 30 degrees, the height of the X-ray source above the disc surface at 10 R_s and the accretion rate at 30% Eddington. Such an accretion rate, which we consider reasonable for an NLS1, results in an ionised disc although we cannot rule out an essentially neutral broad line. A separate narrow Gaussian component ($\sigma = 0.01$ keV) is definitely required to fit the line core, and has an EW of 127 eV. Thus, allowing for a contribution from a broad iron line results in a narrow-line EW similar to that for the narrow-lines in Seyfert 1 galaxies of comparable X-ray luminosity, such as NGC 3783 (Kaspi et al. 2001) and NGC 5548 (Yaqoob et al. 2001).

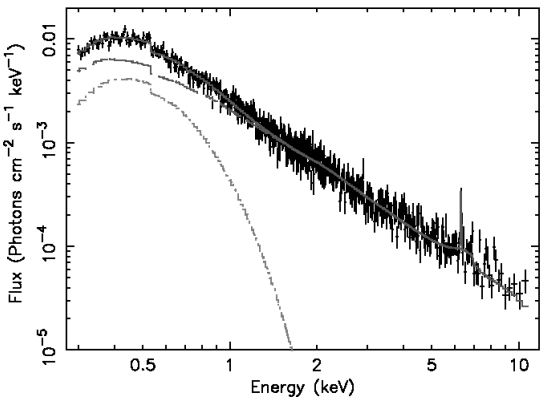

Figure 6. The unfolded 0.2–10 keV EPIC PN spectrum of Mrk 359 fitted using a single blackbody and the ionised accretion disc plus narrow Gaussian emission-line model shown in Fig. 5(b) – fit 5 in Table 2.

Ionised accretion discs, such as that shown in Fig. 5(b), will not only contribute to the iron line but also to the soft X-ray emission due to reflection. This is illustrated in Fig. 6

where we extrapolate the disc model from Fig. 5(b) down to 0.2 keV. Adding a single blackbody to this model provides a good fit to the broadband spectrum (fit 5 in Table 2), removes the need for the hotter blackbody component used in fit 4 in Table 2 and recovers the powerlaw index of the 2–10 keV fit 2 in Table 1.

5 CONCLUSIONS

The *XMM-Newton* spectrum of Mrk 359 reveals a strong iron emission line centred at 6.4 keV. Modelling of the EPIC PN data suggest that this line consists of two components of approximately equal strength: a broad line from an inclined accretion disc and a narrow, unresolved line. Soft X-ray reflection from the ionised disc accretion disc model adopted here also contributes to, but does not completely explain, the broad, soft X-ray excess observed in Mrk 359. Only weak features, due to L-shell absorption in iron M ions, the Ne IX and O VII triplets in emission and O VIII Lyα emission are seen superimposed on the soft X-ray excess. Such soft X-ray excesses have now been clearly detected in a number of broad-line AGN observed by *XMM-Newton*, and may well be ubiquitous (e.g. O'Brien et al. 2001; Reeves et al. 2001; Pounds et al. 2001). It is tempting to ascribe this emission as the high-energy tail of the 'big blue bump' powered by thermal emission from the accretion disc.

A narrow 6.4 keV emission-line seems to be similarly ubiquitous in broad-line AGN (Reeves et al. 2001; Yaqoob et al. 2001; Kaspi et al. 2001; Pounds et al. 2001; Lubinski & Zdziarski 2001). The strength of this line in a fairly low-luminosity AGN like Mrk 359 (with an EW $\approx$ 120 eV) supports the trend, suggested from previous *XMM-Newton* and *Chandra* observations, that the narrow-line is relatively stronger in low compared to high-luminosity AGN. Compared to Mrk 359, NGC 5548 (Yaqoob et al. 2001) and NGC 3783 (Kaspi et al. 2001), the narrow-line is weaker in the luminous Seyfert 1 galaxies, Mrk 205 (Reeves et al. 2001) and Mrk 509 (Pounds et al. 2001), while it is not detected (EW $<$ 10 eV) in the high-luminosity QSOs PKS 0558−504 (O'Brien et al. 2001), S5 0836+710 and PKS 2149−306 (Fang et al. 2001). The narrow-line strength in the lower luminosity AGN implies a significant solid angle (of order π steradian) of cool reprocessing gas lying outside our direct line of sight to the X-ray source. While some of this may be BLR gas (e.g., Yaqoob et al. 2001), the most likely location is the putative molecular torus surrounding the 'central engine' (e.g. Ghisellini et al. 1994).

A straightforward explanation for the correlation of narrow-line strength and luminosity is then that the solid angle subtended by the reprocessing gas declines in high-luminosity AGN, rendering the reflected line difficult to detect. Such a trend would have significant implications for the origin of the reprocessing gas, the relative number of type-1 and type-2 AGN as a function of luminosity and for models seeking to explain the spectral shape of the X-ray background in terms of obscured AGN. For torus models in which the reprocessing gas is a dusty, hydromagnetic wind, the reduction in solid angle may be due to the field lines being 'flattened' by radiation pressure in high luminosity AGN (Konigl & Kartje 1994). Alternatively, Ohsuga & Umemura (2001) suggest that dusty gas-walls supported by radiation pressure from a circumnuclear starburst are more common in relatively low luminosity AGN. Radiation pressure may prevent such walls forming in high luminosity AGN.

Overall, the unusual optical spectrum of Mrk 359 does not translate to an unusual X-ray spectrum. Rather, Mrk 359 has an X-ray continuum and emission-line spectrum consistent with that of a low-luminosity Seyfert 1 galaxy viewed fairly face-on. X-ray spectra for a larger sample of the narrowest-lined AGN are required to determine whether they have systematically different X-ray properties, such as more face-on discs than typical Seyfert 1s or lower/higher accretion rates than for other NLS1s.

ACKNOWLEDGEMENTS

This work is based on observations obtained with the XMM-Newton, an ESA science mission with instruments and contributions diectly funded by ESA member states and the USA (NASA). The authors thank Sergei Nayakshin for providing Xion and for helpful advice on accretion disc models. JR is supported by a Leverhulme Research Fellowship and KP by a Research Studentship from the UK Particle Physics and Astronomy Research Council.

REFERENCES

Boller, T., Brandt, W.N., Fink, H., 1996, A&A, 305, 53
den Herder, J.W. et al., 2001, A&A, 365, L7
Dubus, G., Hameury, J.-M., Lasota, J.-P., 2001, A&A, 373, 251
Elvis, M., Plummer, D., Schachter, J., Fabbiano, G., 1992, ApJS, 80, 257
Davidson, K., Kinman, T.D., 1978, ApJ, 225, 776
Fabian, A.C., Iwasawa, K., Reynolds, C.S., Young, A.J., 2000, PASP, 112, 1145
Fang, T., Marshall, H.L., Bryan, G.L., Canizares, C.R., 2001, ApJ, 555, 356
Ferrarese, L., Pogge, R.W., Peterson, B.M., Merritt, D., Wandel, A., Joseph, C.L., 2001, ApJL, 555, 79
Ghisellini G., Haardt F., Matt G., 1994, MNRAS, 267, 743
Kaspi S. et al. 2001, ApJ, 554, 216
Konigl, A., Kartje, J.F., 1994, ApJ, 434, 446
Lubinski P., Zdziarski A.A., 2001, MNRAS, 323, L37
Nayakshin, S., Kazanas, D., & Kallman, T.R. 2000, ApJ, 537, 833
O'Brien, P.T. et al., 2001, A&A, 365, L122
Ogle, P.M., Marshall, H.L., Lee, J.C., Canizares, C.R., 2001, ApJ, 545, 81
Ohsuga, K., Umemura, M., 2001, A&A, 371, 890
Osterbrock, D.E., Dahari, O., 1983, ApJ, 273, 478
Pounds, K.A., Done, C. Osborne, J., 1995, MNRAS, 277, L5
Pounds K.A., Nandra K., Fink H.H., Makino F. 1994, MNRAS, 267, 193
Pounds, K.A., Reeves, J., O'Brien, P.T., Page, K., Turner, M., Nayakshin, S., 2001, ApJ, in press (astro-ph/0105308)
Reeves, J.N., Turner, M.J.L., Pounds, K.A., O'Brien, P.T., Boller, Th., Ferrando, P., Kendziorra, E., Vercellone, S., 2001, A&A, 365, L134
Sako, M. *et al.* 2001, A&A, 365, L168
Strüder, L. et al., 2001, A&A, 365, L18
Turner, M.J.L. et al., 2001, A&A, 365, L27
Veilleux, S., 1991, ApJ, 368, 158
Walter, R., Fink, H.H., 1993, A&A, 274, 105
Yaqoob, T., George, I.M., Nandra, K., Turner, T.J., Serlemitsos, P.J., Mushotzky, R.F., 2001, ApJ, 546, 759